J. Webster (ed.), *Wiley Encyclopedia of Electrical and Electronics Engineering*

MOBILE RADIO CHANNELS

The term *mobile channel* refers to the transfer function of adio link when one or both of the terminals are moving. The moving terminal is typically in a vehicle such as a car, or a personal communications terminal such as a cellphone. Normally one end of the radio link is fixed, and this is referred to as the base station. In the link, there is usually multipath radiowave propagation, which is changing with time, or more specifically, as a function of position of the moving terminal. The effects of this multipath propagation dominate the behavior and characterization of the mobile channel.

The radio frequency of the link ranges from hundreds of kilohertz, as in broadcast AM radio, to microwave frequencies, as in cellphone communications. Indeed, even optical frequencies are used, as in an infrared link used for indoor computer communications. The kind of channel most often referred to as "mobile," however, is that using microwave frequencies, and this article concentrates on the characteristics of a mobile microwave radio link. Much of the channel behavior can be scaled by the carrier frequency and by the speed of the mobile terminal.

Current spectral usage is a result of many different historical developments, so the bands used by mobile radio channels have evolved to be at many frequencies. For example, current vehicular and personal communications terminals mostly use frequencies around 400 MHz, 900 MHz, and 1.8 GHz. In the future, higher frequencies will be used. The frequency has a definitive bearing on the rate at which the channel changes.

Some examples of mobile channels include: domestic cordless telephones; cellular telephones and radiotelephones; pagers; satellite communication terminals, including navigational services such as Global Positioning System (*GPS*) reception; and radio networks for local data communications. Finally, the reception by portable receivers of broadcast radio, at frequencies of a few hundred kilohertz (AM radio) are common forms of the mobile radio channel.

The use of mobile channels has grown very quickly in the last decade. This growth will continue. It is driven by a combination of consumer demand for mobile voice and data services and advances in electronic technology. A limiting factor to the growth is that many users must share the radio spectrum, which is a finite resource. The spectral sharing is not only local, it is also international, and so spectral regulatory issues have also become formidable. The increasing pressure to use the spectrum more efficiently is also a driving force in regulatory and technical developments.

To a user, a mobile or personal communications system is simple: it is a terminal, such as a telephone, that uses a radio link instead of a wire link. The conspicuous result is that the terminal is compact for portability, and it has an antenna, although for personal communications the antenna is often no longer visible. To the communication engineer, however, the mobile terminal is just a component in a vast, complex circuit. The mobile channel is one link in the circuit, but this link is the most complex, owing to its use of radio waves in complicated propagation environments and of radio signal-processing technology needed to facilitate wireless transmission among multiple users.

In mobile channels, efficient spectral utilization is a function of the basic limitations on controlling radiowave behaor in complicated physical environments, including the launching and gathering of the waves. Thus antennas and propagation are key topics, and their roles characterize the channel behavior.

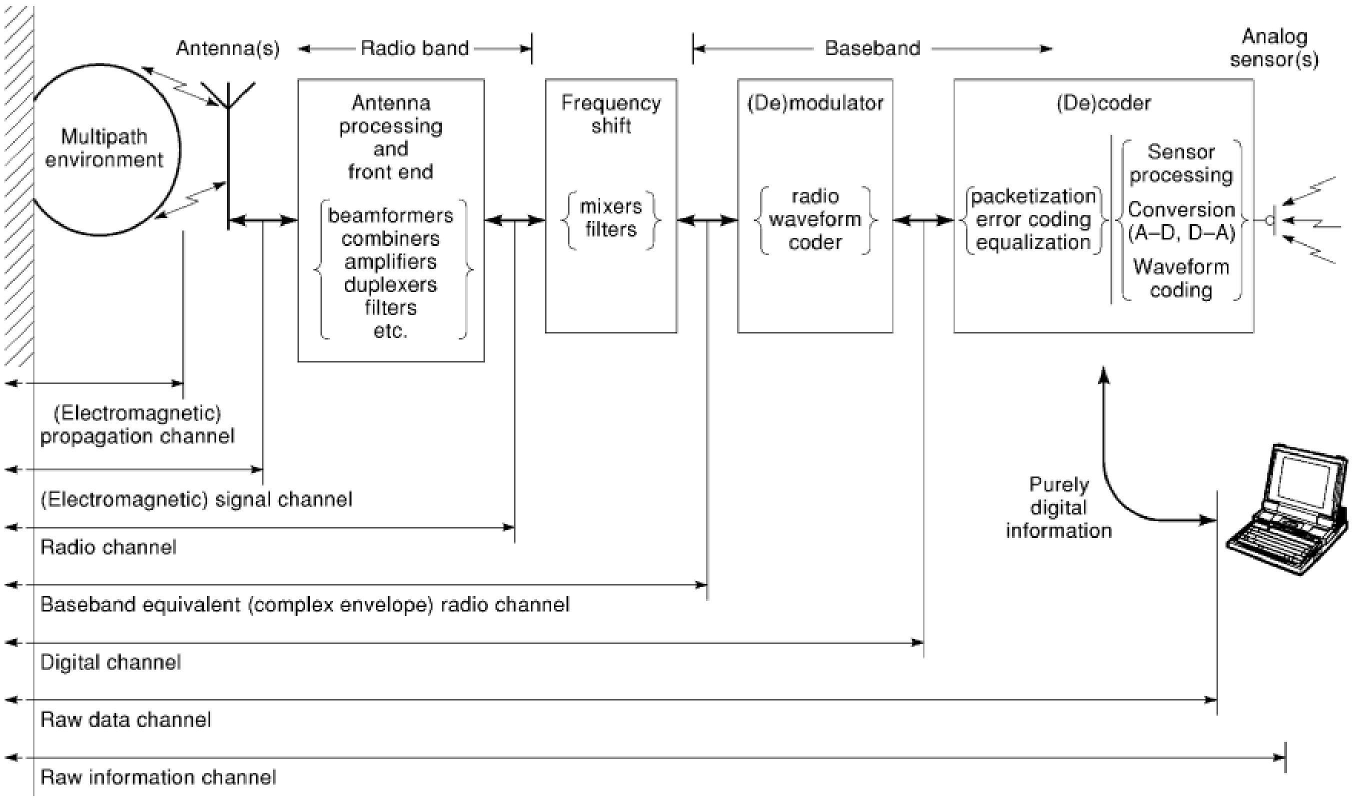

Fig. 1. Various channels in a mobile communications link. The term "mobile channel" refers to the analog aspects of the channel, excluding modulation and coding.

The Mobile Channel

The mobile channel covers many different transfer functions that have different properties. Figure 1 illustrates individual channels (1). The figure shows half of a link, with the other half essentially an inverse process. The multipath propagation environment represents the physical environment of the radio waves in the mobile channel. The flow of information is described here for transmission, but the description adapts readily to reception. A *raw information channel* refers to the transfer function that separates the transmitted and received raw information. For speech, for example, degradations of the immediate acoustical environment from reverberation and acoustic noise form part of the channel "seen" by the user at the receiving end. The quality of the information channel may be subjective, although standard metrics of distortion and signal-to-noise ratio can be applied for characterization. The electrical signal is often digitized for efficient transmission, and the *digital channel* is nonlinear, but its channel quality can be measured directly as a *bit error ratio* (*BER*). This digital form is sometimes rearranged by encoding techniques for more robust transmission of the information. The digital information is coded into analog waveforms and then mixed, or *heterodyned*, to the radio carrier frequency and transmitted via the antenna.

The distinguishing feature of the mobile channel is the changing multipath propagation between transmitter and receiver. The receiving antenna gathers the many incident electromagnetic waves from the multipath environment. These multipath contributions mutually interfere in a random, time-varying manner, and so statistical techniques are needed to characterize the channel. In the physical transmission media, the waves that bear the information are the signals of the *electromagnetic propagation channel*. The antenna reduces the signals from a vector form of orthogonal polarizations to a scalar voltage. The signal at the open circuited receiving antenna terminal is the output of the *electromagnetic signal channel*. The antenna needs to be terminated in order to maximize the power received by the front end. The signal-to-noise ratio (*SNR*) is established at this point in the link, and the resulting signal is the output of the *radio channel*. The antenna is a critical part of the mobile channel, and it can control much of the channel behavior. The baseband equivalent form of the radio channel, which is the radio channel shifted in frequency to a low-pass spectral position, is the signal that engineers use for mathematical characterization and most electronic (including digital) signal processing. The analog form of the radio channel is what will be referred to from here on as the mobile channel.

Multiple Access for Mobile Channels. Most mobile communications systems are for multiple users, and a *multiple access* technique is required to allow the spectrum to be shared. In cellular systems, for example, the frequencies are reused at geographically spaced locations. For indoor systems, the frequency reuse spacing may be between floors. In a system design, the multiple access technique interacts with the choice of channel modulation and signal coding. The three basic techniques are frequency division multiple access (*FDMA*), which has channels occupying different narrow bandwidths simultaneously; code division multiple access (*CDMA*), in which multiple users share wider bandwidths simultaneously by using differently coded waveforms; and time division multiple access (*TDMA*), in which users share a bandwidth by occupying it at multiplexed times. Some systems employ a combination of these techniques.

Multiple access is not a part of the mobile channel as such. However, the reader should remain aware that multiple access is part of the communations system and the choice of technique has an influence on the mobile channel bandwidth, its usage, and the type of signaling employed. Multiple access also brings in co- and adjacent-channel interference, in which the unwanted signals at a receiver may not be noiselike, but in fact be signals with very similar characteristics to the wanted signal. In systems with densely packed users, the system capacity is interference-limited.

Multipath Propagation Effects

Multipath radiowave propagation is the dominant feature of the mobile channel. More often than not, the transmitted signal has no line-of-sight path to the receiver, so that only indirect radiowave paths reach the receiving antenna. For microwave frequencies, the propagation mechanisms are a mixture of specular (i.e., mirrorlike) reflection from electrically smooth surfaces such as the ground, walls of buildings, and sides of vehicles; diffraction from edges of buildings, hills, etc.; scattering from posts, cables, furniture, etc.; and diffuse scattering from electrically rough surfaces such as some walls and grounds.

Some multipath propagation occurs in nearly all communications links. The basic phenomenon is that several replicas of the signal are received, instead of one clean version. The result can be seen as television ghosts, for example. On transmission lines, reflections from mismatches on the line give the same effect, for example, echoes on telephone lines. On a long distance point-to-point radio link, a direct line-of-sight wave, a single ground bounce, and atmospherically refracted waves can all contribute to the received signal. When signal replicas are too close together to be discriminated and processed as discrete contributions, the received signal becomes distorted. This distortion limits the capacity of the channel. The phenomena is akin to the severe acoustic distortion known as the *railway station effect*, where increasing power output (volume) does not increase the intelligibility of the message. In digital communications, the distortion caused by multipath propagation creates an analogous effect: an increase in transmitted power does not decrease the BER as Shannon's theorem might suggest. The amount and nature of the multipath propagation sets the level of power at which the BER becomes essentially independent of the SNR. The effect has often been referred to as the "irreducible BER," but the use of signal processing, in particular equalization, can in fact reduce the BER further. Experimental examples of the irreducible BER in the digital channel are given below, but this article otherwise concerns the analog mechanisms and the statistical nature of the mobile channel.

Fading in the Mobile Channel.

Fast Fading. The interference, or phase mixing, of the multipath contributions causes time- and frequency-dependent fading in the gain of the channel. The time dependence is normally from the changing position of the mobile terminal, and so is also referred to as space dependence. At a given frequency, the power of the received signal, and thus the gain of the mobile channel, changes with time. This changing SNR is called *signal fading* and is often experienced as audible "swooshing" or "picket fencing" when an FM station (with a radio frequency of about 100 MHz) is received by the antenna on a moving car. If the mobile terminal is stationary, the signal may continue to experience some fading, and this is caused by changes in the multipath environment, which may include moving vehicles, etc.

In nearly all situations the changing mobile position dominates the time variation of the mobile channel. Usually, the multipath environment is taken, or at least modeled, as unchanging. This is called the *static multipath* assumption. In this case, a static mobile experiences an unchanging channel. If now the radio frequency is swept, then the gain of the transfer function experiences fading similar to that due to changes in position, because the electrical path distances of the multipath components are frequency-dependent. For a continuous wave (*CW*) signal, the time- and frequency-dependent fades can be some 40 dB below the mean power level, and up to 10 dB above the mean. This indicates the large dynamic range required of the receiver just to handle the multipath interference. This fading is variously called the *fast fading*, or *short term fading*, or *Rayleigh fading* after the Rayleigh distribution of the signal magnitude. The maximum density of fading is a fade about every half wavelength on average, and this occurs typically in urban outdoor environments. The fast fading dominates the mobile channel characteristics and usage. For example, amplitude modulation at microwave frequencies is not feasible, because for a fast-moving mobile terminal the fading interferes directly with the modulation.

Slow Fading. The dynamic range of the received signal is also affected by *slow fading*, also called *long term fading* or *shadow fading*. This is superimposed on the fast fading. It is caused by shadowing of the radio signal to the scatterers as the mobile terminal moves behind large obstacles such as hills and buildings. The rate of the slow fading therefore depends on the large scale nature of the physical environment. The basic short term multipath mechanism remains unchanged. The dynamic range of the slow fading is typically less than that of the fast fading, being confined to about ± 10 dB for most of the time in urban and suburban environments. The total dynamic range for the fading therefore becomes about 70 dB. The distance-based path loss, as a mobile terminal roams near to and far from a base station, adds to this range.

Narrowband and Wideband. In a typical mobile microwave signal link, the *relative bandwidth* is small. This means that the spectral extent of the signal is less than a few percent of the nominal carrier frequency. The fading within the frequency response of the transfer function is referred to as *frequency-selective fading*. If the bandwidth is sufficiently small so that all the frequency components fade together, then this is called a *flat fading* channel.

In the mobile channel context, a *narrowband* channel has flat fading and a *wideband* channel has frequency-selective fading. The use of a single frequency, or CW, for channel characterization is the limiting case of the narrowband channel. Historically, fading has been the principal observed characteristic of the mobile channel. Fast fading is merely one manifestation of the reception of several replica signals.

The Effect of Fading on the Digital Channel: Irreducible Bit Error Ratio.

Timing Errors From Random Frequency Modulation. The digital channel in Fig. 1. is in principle the simplest channel to characterize experimentally, since it concerns a BER measure. The fading in the mobile channel has a particular effect on the BER curves, namely, the "irreducible BER" mentioned above. The example in Fig. 2. (2) shows curves of BER against carrier-to-noise ratio (*CNR*) from simulations of the narrowband mobile channel with carrier frequency 920 MHz. The static (no fading) curve shows the classical waterfall shape of the Gaussian channel. But the fading channel curves, shown with fading rate f_{D}, feature irreducible

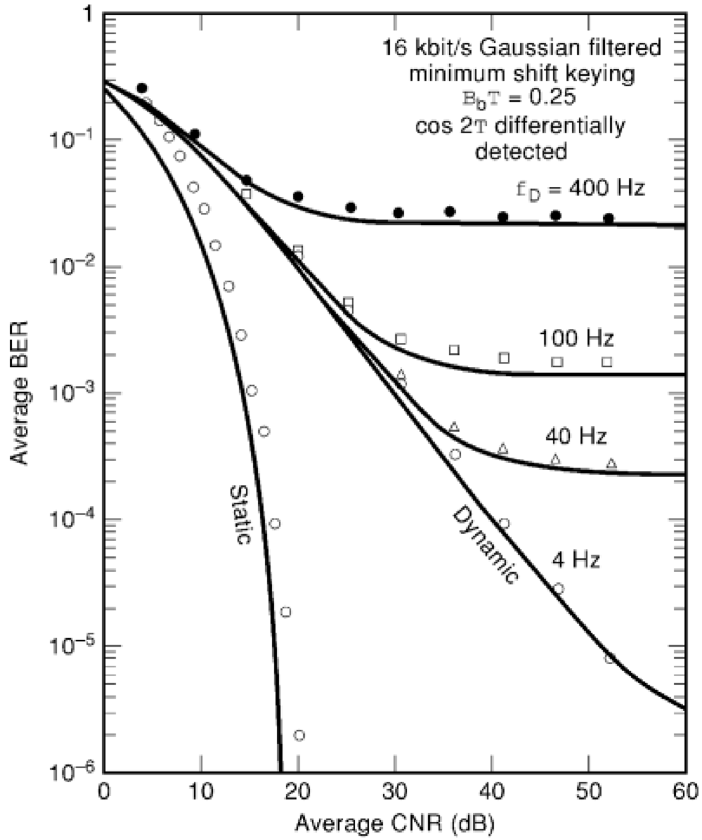

Fig. 2. The irreducible BER for a digital mobile channel is attained when an increase of SNR does not improve the BER. The static (no fading) channel shows the classical waterfall shape of the Gaussian noise-limited channel, but as the fading rate increases, the form of the curve alters drastically. From 2.

BERs, which occur at lower CNRs with increasing fading rate. The fading rate of 40 Hz corresponds to a mobile speed of about 40 km/h and a carrier frequency of 900 MHz. This corresponds approximately with using a cellphone from a moving car. The curves hold their basic form independently of the type of angle modulation used. The mechanism for the bit errors is timing error caused by the random FM, discussed below, imposed on the signal by the fading channel. The random FM causes jitter on the symbols after they passed through the mobile channel.

Intersymbol Interference From Multiple Time Delays. As the signaling rate increases, an analogous irreducible BER effect occurs as a result of the several signal replicas arriving at different times. This spread of delays causes intersymbol interference when one dispersed symbol overlaps with other, similarly dispersed symbols. In analog parlance, this is called dispersive distortion. In the mobile channel the situation is complicated by the dispersion changing with time. The effect is depicted in the experimental example of Fig. 3. (3), where for a fixed fading rate of $f_D = 40$ Hz the increasing digital transmission rate experiences an increasing irreducible BER. As in Fig. 2, the effect is that the capacity of a given link cannot be increased by simply increasing the CNR, for example, by increasing the transmitted power. Signal processing is required.

Signal Processing for Mitigation of the Multipath Effect. Several signal-processing techniques can be applied to the mobile channel to reduce distortion and recover the capacity relative to the static channel.

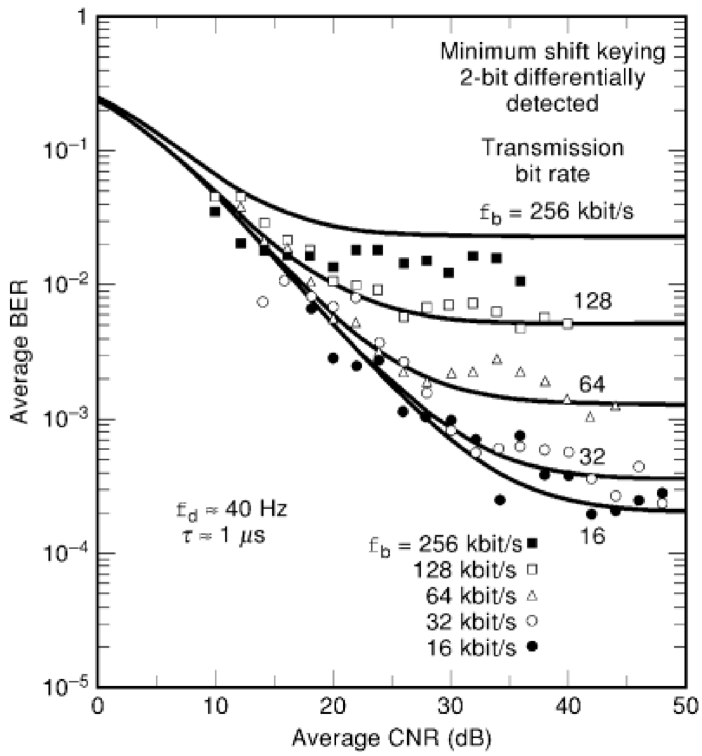

Fig. 3. The irreducible BER caused by intersymbol interference. As the fading rate increases relative to the spread of multipath propagation delay times, the irreducible BER increases. From 3.

Equalization and *rake* systems basically attempt to gather the delayed signal replicas and recombine them into a single signal, which, ideally, is no longer distorted or faded. *Antenna diversity* uses multiple antenna elements to receive the same signal but with different multipath degradations, and combines the signals so that the resultant channel has better capacity than any of the channels from the individual antenna elements. A combination of the equalization, or rake, and antenna diversity methods is called *space-time processing*. All these techniques can be effective in improving the mobile channel. In fact, the use of antenna diversity offers very large potential capacities by effectively reusing the frequency at different positions in space.

The Mobile Channel as a Transfer Function. Figure 4 depicts a static mobile channel, which is taken as the baseband equivalent radio channel of Fig. 1. Recall that the effect of the antennas is included in the transfer function. The impulse response $h(\tau)$ and the transfer function $H(\omega)$ are related by Fourier transformation in the usual way, denoted $h(\tau) \iff H(\omega)$. Here τ is the delay time and ω is the angular baseband equivalent frequency. The impulse response indicates the dispersive nature of the channel, which causes distortion of the signals which are transmitted through it. This impulse response is modeled as a series of discrete delta functions below.

The example of Fig. 1 is for an instant in time, t. As the mobile terminal moves, the delays and phases of the individual multipath contributions become functions of time. The impulse response and transfer function therefore become expressed mathematically as functions of time, that is, $h(\tau, t)$ and $H(\omega, t)$. If the scatterers in the multipath environment can be considered to be essentially stationary, then the time t and position z are related by the velocity V of the mobile: $z=Vt$. From now on the spatial variable z will be mostly used.

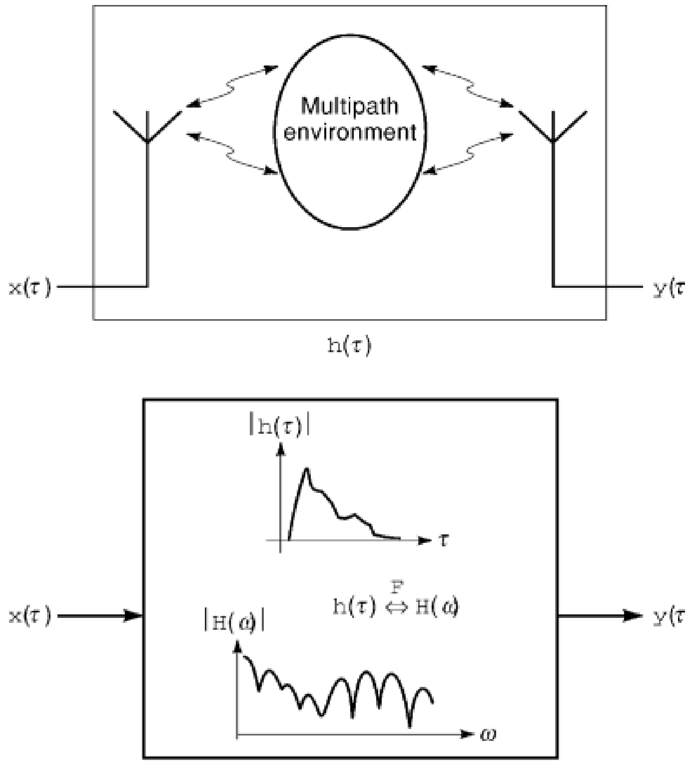

Fig. 4. The static mobile channel transfer function. $x(\tau)$ and $y(\tau)$ are electronic signals before the transmitting antenna and after the receiving antenna, respectively. The impulse response can be found by Fourier transformation of a swept frequency measurement, for example.

The following sections will develop, through the use of several assumptions about the channel, a double Fourier transform relation between the impulse response as a function of delay time and time (i.e., position) and the transfer function as a function of baseband angular frequency and Doppler frequency. Because of the variation of the transfer functions, the statistical parameters of the channel are relevant, and these also can be couched in terms of Fourier relations.

The Receiving Antenna in Multipath Transmission. The moving antenna combines the radiowave contributions, which have continuously changing delays, amplitudes, and polarizations. Deterministic analysis is not feasible except in simplistic situations, and to be able to interpret the statistical description requires an appreciation of multipath phenomena.

A base station transmitter is taken to emit power in a fixed radiation pattern. After multiple scattering, for example from many reflections, the polarization is changed in a random way and the electric (and magnetic) field has all three Cartesian components, independent of the transmitted polarization. These components can be independent functions of frequency and position. So the total incident electric field, at a point in space, can be written in baseband equivalent form [i.e., with a complex envelope, in which a factor of $\exp(j\omega_C\, t)$ is suppressed, where ω_C is the carrier frequency] as the complex vector

$$\begin{aligned} \boldsymbol{E}_{\mathrm{I}}(\omega;\, x,\, y,\, z) = \boldsymbol{E}_x(\omega;\, x,\, y,\, z)\hat{\boldsymbol{x}} + \boldsymbol{E}_y(\omega;\, x,\, z)\hat{\boldsymbol{y}} \\ + \boldsymbol{E}_z(\omega;\, x,\, y,\, z)\hat{\boldsymbol{z}} \end{aligned} \tag{1}$$

in which the components, such as E_{x}, are complex scalars.

The introduction of an antenna promotes a change to spherical coordinates referred to the antenna orientation and position. The position is denoted with the single spatial variable z. The incident fields are now written as

$$E_1(\omega,\, z;\, \theta, \phi) = E_\theta(\omega,\, z;\, \theta, \phi)\hat{\theta} + E_\phi(\omega,\, z;\, \theta, \phi)\hat{\phi} \qquad (2)$$

The open circuit voltage of an antenna depends on both the incident field and the receiving pattern, $\boldsymbol{h}_{\mathrm{a}}(\omega\ \theta, \phi) = h_\theta(\omega\ \theta, \phi)\hat{\theta} + h_\phi(\omega\ \theta, \phi)\hat{\phi}$. This notation for the receiving pattern should not be confused with the symbol for the impulse response, $h(\tau{,}z)$. The open circuit voltage is defined by

$$V_O(\omega,\, z) = \int_0^{2\pi}\int_0^{\pi} E_1(\omega,\, z;\, \theta,\, \phi) \cdot h_a(\omega; \theta, \phi) \sin\theta\, d\theta\, d\phi \quad (3)$$

and represents the transfer function of the electromagnetic signal channel.

By expanding the dot product, this transfer function is written in terms of the incident field components, which are now collectively detected as *standing waves*, and the receiving pattern components, as

$$\begin{aligned} H(\omega,\, z) = \int_0^{2\pi}\int_0^{\pi} &[E_\theta(\omega,\, z;\, \theta,\, \phi) h_\theta(w; \theta\phi) \\ &+ E_\phi(\omega,\, z,\, \theta, \phi) h_\phi(\omega; \theta,\, \phi)] \sin\theta\, d\theta\, d\phi \end{aligned} \qquad (4)$$

This formula shows the inseparability of the antenna pattern and the incident fields in the definition of the mobile channel. The antenna pattern is recognized as a filter in the spatial (including polarization) domain. The frequency dependence of the antenna pattern also represents a filter in the more familiar frequency domain. The space–frequency filter of the antenna is the difference between the vector electromagnetic propagation channel and the scalar electromagnetic signal channel of Fig. 1. If terminating (i.e., matching) the antenna has a negligible effect over the band of interest, then Eq. (4) represents the mobile channel.

Channel Model using Discrete Effective Scatterers

Modeling the incident waves as emanating from discrete directions allows the convenience of using effective point sources. These are referred to as *effective scatterers*, because their scalar contribution is the physical incident wave weighted by the receiving pattern. The transfer function is written as the sum of effective scatterers, which have an amplitude a, a phase ψ and a delay time τ for the information carried, that is,

$$H(\omega, z) = \sum_i a_i\ \exp(j\psi_i)\ \exp(-j\omega_{\mathrm{R}}\tau_i) \qquad (5)$$

Here the radio frequency is the sum of the carrier frequency (the center frequency of the radio band) and baseband equivalent frequency, i.e.,

$$\omega_{\mathrm{R}} = \omega_{\mathrm{C}} + \omega \qquad (6)$$

In the static situation, the terms in the transfer function containing the delays are constant and can be incorporated into the phases of the effective scatterers.

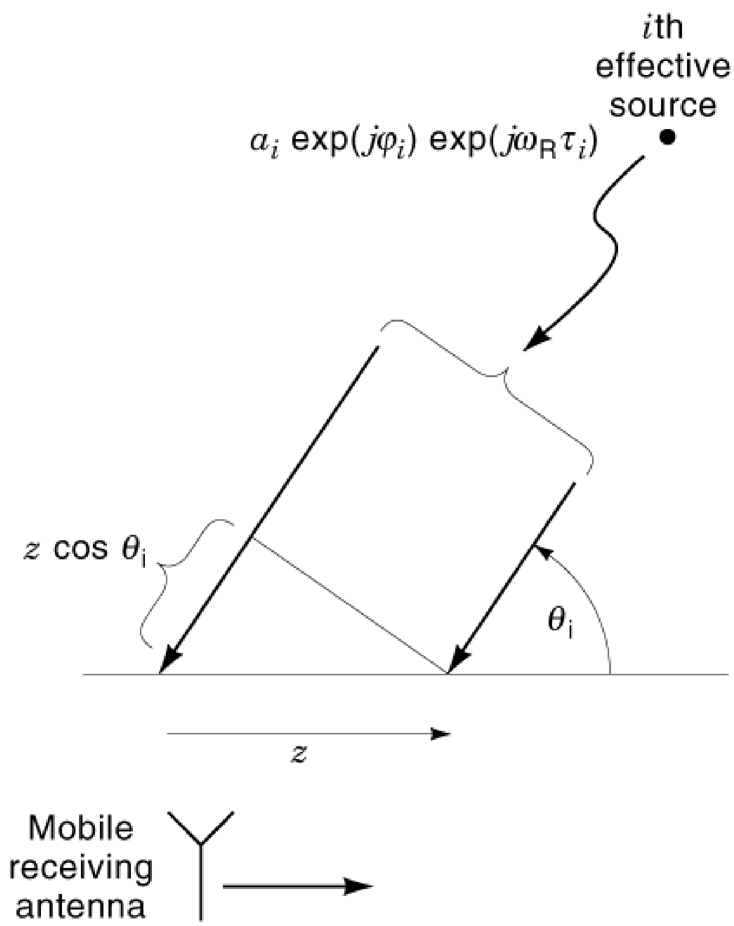

Fig. 5. Point source with moving receiver. In a model of the channel, Eq. (5), the point source is not necessarily a physical scatterer, but can rather be considered as a point representation (an "effective scatterer") that produces the waves received from a given angular direction.

The effect of the moving terminal on the transfer function can be seen by considering an effective scatterer at a relatively large distance r_0 from it. The geometry is shown in Fig. 5. The mobile terminal moves a distance z along the spatial axis in the positive direction. The electrical distance to the i th effective scatterer changes from $k_R\ r_{\theta i}$, where k_R is the radio frequency wavenumber, to

$$\begin{aligned} k_R r_i &\approx k_R r_{0i} - k_R z\ \cos\ \theta_i \\ &= \omega_R \tau_i - \frac{\omega_R}{c} \cos \theta_i\, z \\ &= \omega_R \tau_i - u_i z \end{aligned} \tag{7}$$

where

$$u_i = k_R\ \cos\ \theta_i \tag{8}$$

is the *spatial Doppler frequency* in radians per meter. The Doppler frequency in radians per second is

$$\omega_{Di} = u_i V = k_R V\ \cos\ \theta_i \tag{9}$$

Here u_i is a scaled directional cosine to the ith effective scatterer, and a receiver movement z produces a phase shift uiz in the signal from the scatterer.

The changing phase term of an effective scatterer at position z in Eq. (5) is

$$\omega_R \tau_i = \omega_C \tau_i + \omega \tau_i - \frac{\omega_C}{c} \cos \theta_i z - \frac{\omega}{c} \cos \theta_i z \qquad (10)$$

The first term is independent of the position and baseband frequency, and can be incorporated in the phase of the scatterer. The last term is negligible, because in microwave communications we normally have a small relative bandwidth (i.e., $\omega/\omega_C \ll 1$). So within the above approximations, the transfer function is

$$H(\omega, z) = \sum_i a_i \exp(j\psi_i) \exp[j(-\omega\tau_i + zu_i)] \qquad (11)$$

Fourier transformation with respect to the baseband frequency ω gives the position-dependent impulse response as a function of the delay time and position,

$$h(\tau, z) = \sum_i a_i \exp(j\psi_i)\,\delta(\tau - \tau_i) \exp(ju_i z) \qquad (12)$$

A further Fourier transformation, this time with respect to the position z, gives a function of delay time and spatial Doppler frequency, denoted

$$a(\tau, u) = \sum_i a_i \exp(j\psi_i)\,\delta(\tau - \tau_i)\, 2\pi\delta(u - u_i) \qquad (13)$$

Fourier Transform Relations With Continuous Transfer Functions. The Fourier pair $a(\tau,u) \Longleftrightarrow H(\omega,z)$ have the continuous form

$$H(\omega, z) = \frac{1}{2\pi} \int_0^{\infty} \int_{-k_C}^{k_C} a(\tau, u) \exp[j(-\omega\tau + zu)]\, du\, d\tau \qquad (14)$$

$$a(\tau, u) = \frac{1}{2\pi} \int_{-\infty}^{\infty} \int_{-\infty}^{\infty} H(\omega, z) \exp[j(\omega\tau - zu)]\, d\omega\, dz \qquad (15)$$

Note the mixed signs of the exponents. Moving in the negative z direction instead of the positive z direction, for example, changes the sign of the exponent zu in Eqs. (14) and (15).

From the double Fourier transform relation, there can be four complex functions that carry the same information for characterization of the mobile channel. These are denoted:

a (τ, u), the scattering function in the time-delay–spatial-Doppler domain (referred to as the effective scattering distribution)

h (τ, z), the impulse response in the delay–space domain (spatial spectrum)

A (ω, u), the transfer function in the baseband-frequency–spatial-Doppler domain (frequency spectrum)

H (ω, z), the transfer function in the baseband-frequency – domain (space–frequency spectrum)

The functions are related by the following single-dimensional Fourier transforms of the mobile channel:

$$a(\tau, u) = \frac{1}{2\pi}\int A(\omega, u)e^{j\omega\tau}\,d\omega, \qquad A(\omega, u) = \int a(\tau, u)\,e^{-j\omega\tau}\,d\tau \tag{16}$$

$$h(\tau, z) = \frac{1}{2\pi}\int H(\omega, z)e^{j\omega\tau}\,d\omega, \qquad H(\omega, z) = \int h(\tau, z)\,e^{-j\omega\tau}\,d\tau \tag{17}$$

$$a(\tau, u) = \int h(\tau, z)e^{-jzu}\,dz, \qquad h(\tau, z) = \frac{1}{2\pi}\int a(\tau, u)\,e^{jzu}\,du \tag{18}$$

$$A(\omega, u) = \int H(\omega, z)e^{-jzu}\,dz, \qquad H(\omega, z) = \frac{1}{2\pi}\int A(\omega, u)\,e^{jzu}\,du \tag{19}$$

The amplitudes, phases, delays, and directions of the effective sources are randomly distributed, and the transfer function consequently behaves randomly, so a statistical approach is called for their characterization.

Averaging Across a Transfer Function For Channel Gain. In terms of an individual channel transfer function, the total power, or *channel gain*, is given by

$$P^{(\mathrm{i})} = \frac{1}{L\omega_{\mathrm{B}}}\int_L\int_{\omega_{\mathrm{B}}} |H(\omega, z)|^2\,d\omega\,dz \tag{20}$$

where L is an averaging distance or locus covering the positional averaging, and ω_{B} is an averaging bandwidth. Any of the above channel functions can be used to get the power in this way (Parseval's theorem). Integrating single variables gives the frequency-dependent power transfer function averaged over position,

$$|H(\omega)|^2 = \frac{1}{L}\int_L |H(\omega, z)|^2\,dz \tag{21}$$

and the position-dependent- (time-dependent)- power transfer function averaged over the frequency band,

$$|H(z)|^2 = \frac{1}{\omega_{\mathrm{B}}}\int_{\omega_{\mathrm{B}}} |H(\omega, z)|^2\,d\omega \tag{22}$$

This quantity is approximated in a receiver by the position-varying (or time-varying) received signal strength indicator (*RSSI*) signal. However, in practice, the RSSI voltage is normally proportional to the logarithm of the channel power.

On averaging the power across a wideband channel, the total received power fades less than a narrowband component. This is the advantage of wideband modulation systems. Analogously, antenna diversity is used to reduce the fading by averaging the channel over samples of the spatial variable.

Statistical Basis of a Mobile Channel

Power Spectra and Channel Correlation Functions. Assuming ergodicity so that the statistics remain second order, the *autocorrelation function*, denoted by R, of the effective scatterer distribution with respect to the delay times is written

$$R_a(\tau_1, \tau_2;\, u) = \langle a(\tau_1, u)a^*(\tau_2, u)\rangle \qquad (23)$$

where the angular brackets denote averaging over all relevant realizations of the effective scattering distribution. This contrasts with the averaging over frequency or space for a single channel realization as in the previous section. The average power in the effective scattering distribution is

$$P(\tau, u) = R_a(\tau, \tau;\, u) = \langle |a(\tau, u)|^2\rangle \qquad (24)$$

Note that the averaging is of the powers, not of the complex values, of the $a(\tau, u)$.

This averaged power distribution can be expressed in several different statistical forms as seen below. Substituting Eq. (16) into Eq. (23) gives the Fourier transform

$$\begin{aligned} &R_a(\tau_1, \tau_2; u) \\ &\quad = \frac{1}{4\pi^2}\int_{-\infty}^{\infty}\int_{-\infty}^{\infty} R_A(\omega_1, \omega_2; u)\exp[j(\omega_1\tau_1 - \omega_2\tau_2)]\,d\omega_1 d\omega_2 \end{aligned} \qquad (25)$$

The inverse relation is

$$\begin{aligned} &R_A(\omega_1, \omega_2; u) \\ &\quad = \int_0^{\infty}\int_0^{\infty} R_a(\tau_1, \tau_2; u)\exp[-j(\omega_1\tau_1 - \omega_2\tau_2)]\,d\tau_1 d\tau_2 \end{aligned} \qquad (26)$$

Wide Sense Stationarity in Frequency. The channel is now assumed to be *wide sense stationary in the frequency domain*. This means that the mean and correlation of $A(\omega, u)$ do not depend on the choice of frequency, ω, but on only the frequency difference, $\Delta\omega = \omega_2 - \omega_1$. This is a reasonable assumption for the frequencies within the small relative bandwidths of most mobile communications systems. Denote the autocorrelation of a wide sense stationary (*WSS*) process using S, for example, by

$$R_A(\omega_1, \omega_2; u) = R_A(\omega, \omega + \Delta\omega; u) = S_A(\Delta\omega; u) \qquad (\text{WSS in } \omega) \qquad (27)$$

i.e., the autocorrelation of the transfer function in the frequency–spatial-Doppler domain is a power spectrum whose argument is the frequency difference. The symbols S and R are used to represent the correspondence of the power spectra S and the autocorrelation R of a process that is WSS. As a result of the wide sense stationarity in ω, we can write Eq. (25) as

$$R_a(\tau_1, \tau_2; u) = \frac{1}{4\pi^2} \int \int S_A(\Delta\omega; u) \exp(-j\,\Delta\omega\tau_2) \exp[-j\omega_1(\tau_2 - \tau_1)] d\omega_1 d\Delta\omega = P(\tau_2, u)\delta(\tau_2 - \tau_1) \tag{28}$$

where

$$P(\tau, u) = \frac{1}{2\pi} \int_{-\infty}^{\infty} S_A(\Delta\omega, u)\ \exp(j\ \Delta\omega\ \tau)\ d\Delta\omega \tag{29}$$

is the averaged power delay–Doppler-frequency distribution of Eq. (24). The delta function in the autocorrelation of Eq. (28) is referred to as the *uncorrelated scattering* (*US*), and here means that a fading signal received at a given delay time is uncorrelated (when averaged over the relevant realizations) with a fading signal received at any other delay time. The wide sense stationarity (via the $\Delta\omega$ factor) in the baseband frequency domain and the uncorrelated scattering in the delay time domain [the $\delta(\Delta\tau)$ factor] are equivalent characteristics.

Wide Sense Stationarity in Space. Similarly, *wide sense stationarity in the spatial domain* corresponds to uncorrelated scattering in the Doppler domain. This means that the fading signal at one spatial Doppler frequency u [or angle $\theta = \cos^{-1}(u/k_C)$] is uncorrelated with a fading signal received from any other spatial Doppler frequency. Denoting the spatial difference $\Delta z = z_2 - z_1$, we have

$$R_a(\tau; u_1, u_2) = \iint S_h(\tau;\ \Delta z)\ \exp[j(z_2u_2 - z_1u_1)]\ dz_1\ dz_2 = P(\tau, u_2)\, 2\pi\,\delta(u_2 - u_1) \tag{30}$$

where the averaged power of the effective scattering distribution is expressed as

$$P(\tau, u) = \int S_h(\tau, \Delta z)\ \exp(-j\ \Delta z\ u)\ d\Delta z \tag{31}$$

Wide Sense Stationary Uncorrelated Scattering Channel. Combining the space and frequency wide sense stationarity conditions, we have

$$\begin{aligned} &R_a(\tau_1, \tau_2; u_1, u_2) \\ &\quad = \frac{1}{2\pi} \iint S_H(\Delta\omega, \Delta z)\ \exp[j(-\Delta\omega\,\tau_2 + \Delta z\, u_2)] \\ &\qquad d\Delta\omega\ d\Delta z \delta(\tau_2 - \tau_1)\ 2\pi\,\delta(u_2 - u_1) \\ &\quad = P(\tau_2, u_2)\,\delta(\tau_2 - \tau_1)\, 2\pi\,\delta(u_2 - u_1) \end{aligned} \tag{32}$$

where now

$$P(\tau, u) = \frac{1}{2\pi} \int \int S_H(\Delta\omega, \Delta z)\ \exp[-j(\Delta\omega\,\tau - \Delta z\ u)]\, d\Delta\omega\, d\Delta z \tag{33}$$

The inverse Fourier transform is

$$S_H(\Delta\omega, \Delta z) = \frac{1}{2\pi} \int\int P(\tau, u)\ \exp[j(\Delta\omega\,\tau - \Delta z\, u)]\, d\tau\, du \quad (34)$$

Thus the above wide sense stationarity conditions result in the frequency–space correlation function being the double Fourier transform of the average power density of the effective scatterer distribution.

The term WSSUS was used by Bello (4) to describe tropospheric multipath channels containing scintillating scatterers being illuminated by static antennas. In the context of the mobile channel, the WSS refers to wide sense stationarity in position, which implies uncorrelated scattering in the spatial Doppler frequency. The US refers to the delta function in delay time (effective sources at different delays are mutually uncorrelated), which implies WSS in the frequency domain.

The assumption of the WSSUS conditions in the channel allows the convenience of the double Fourier transform relations. However, in applying the Fourier relations for a given situation, the validity of the WSSUS model should always be questioned. The channel can often be arranged to be "sufficiently valid" for gaining useful insight and inferring channel behavior, by appropriately arranging the averaging. This averaging, denoted with the angular brackets, is often taken as several sampled records over short distances (tens of carrier wavelengths or several tens of fades) in order to stay within a given physical environment, followed by the power distribution averaging. Statistically, ensemble averaging implies many "realizations." We can interpret this as several sampled records that should have uncorrelated data (e.g., well separated spatial paths) within the same physical environment, or else as several records in different (i.e., independent) physical environments. The two cases are different. One case averages within a single environment; the other case averages over many different environments. Strictly speaking, the presence of multiple uncorrelated records in the same immediate environment does not truly satisfy the hypothesis of statistically independent records, because the scattering distribution is the same, that is, the signal sources constituting the physical scatterers are common to all the data records.

Key Relations For a Mobile Channel. Equations (14), (15) and ((33), (34) are key results for the mobile channel. They relate, respectively, by double Fourier transformation, a baseband channel transfer function $H(\omega, z)$ to an effective source distribution $a(\tau, u)$ that provides the incident multipath signals, and the average power spectral density of the channel $S_H(\Delta\omega, \Delta z)$ to the average power distribution of the effective scatterers, $P(\tau, u)$ Figure 6 (1) depicts the relations between the functions.

Averaged Power Profiles. The more familiar single transformations also are of interest. Mathematically, we can put $\Delta z = 0$ in the frequency correlation, that is,

$$S_H(\Delta\omega) = S_H(\Delta\omega, \Delta z = 0) = \langle H(\omega, z_0) H^*(\omega + \Delta\omega, z_0)\rangle \quad (35)$$

from which Eq. (34) reduces to

$$S_H(\Delta\omega) = \int P(\tau)\ \exp(-j\ \Delta\omega\ \tau)\, d\tau \quad (36)$$

where the average power delay profile,

$$P(\tau) = \int P(\tau, u)\, du \quad (37)$$

is the average power at delay τ, found by integrating over all spatial Doppler frequencies ($u = k_C$ to $u = -k_C$), that is, in all directions over the averaged power of the effective scattering distribution. In practice, the

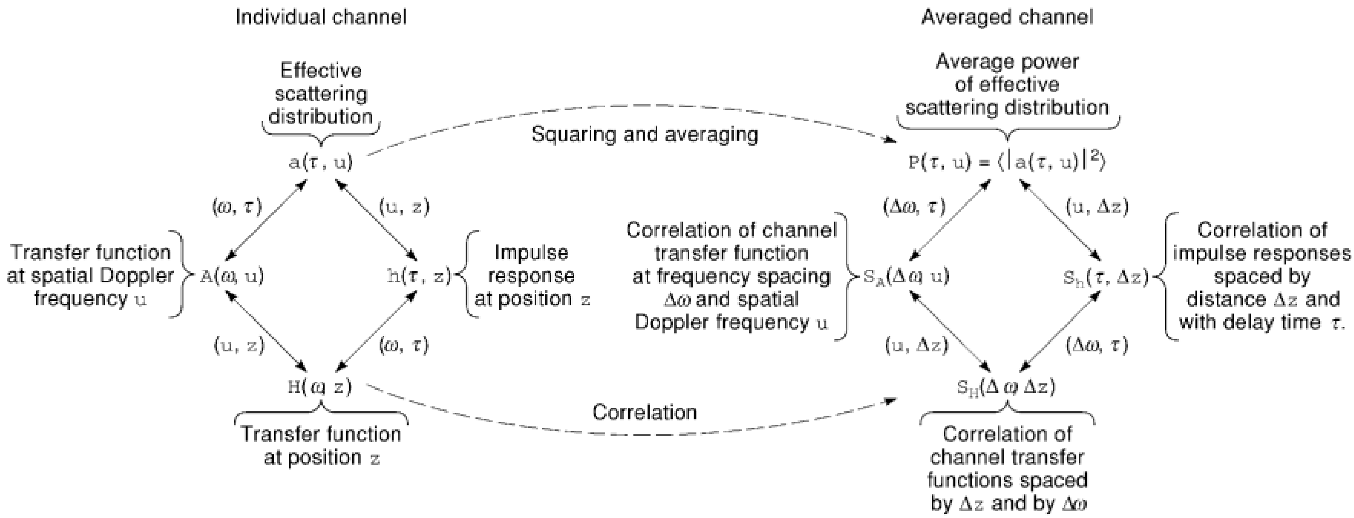

Fig. 6. Fourier transform relations for the mobile channel functions and for their statistical representations under wide sense stationarity in frequency and position. $u = k_C \cos\theta$ is the spatial Doppler frequency, with θ the zenith angle with respect to the direction of motion z, and k_C the wavenumber of the radio carrier frequency. From Ref. 3.

antenna performs this integration [recall that the effective scattering distribution $P(\tau, u)$ already includes the effect of the antenna] for example, an omnidirectional antenna will gather the waves from all the directions. However, a single measurement from an antenna only accounts for a single realization of the effective scattering distribution—that is, for one point in the space of one environment. To estimate $P(\tau)$ from measurements, the averaging of the profile needs to be done over several different positions [i.e., several z_0 values in Eq. (35)], either in the same physical environment or in many different physical environments, as discussed above.

The frequency correlation function $S_H(\Delta\omega)$ is the Fourier transform of the average power delay profile $P(\tau)$ for the WSS channel with uncorrelated scattering. The inverse relation is

$$P(\tau) = \frac{1}{2\pi} \int S_H(\Delta\omega)\ \exp(j\ \Delta\omega\ \tau)\ d\Delta\omega \qquad (38)$$

The Fourier relation in Eqs. (36) and (38) is identical to the relation between the transfer function and its impulse response, as in Fig. 4.

Similarly to the average delay profile, *the average spatial Doppler profile* is averaged over all delays:

$$P(u) = \int P(\tau, u)\, d\tau \qquad (39)$$

$P(\tau)$ and $P(u)$ are sometimes called the delay spectrum and the Doppler spectrum respectively. Finally, the total power of the effective scatterers is given by

$$P = \int \int P(\tau, u)\, d\tau\, du \qquad (40)$$

Many details, extending to situations outside the mobile channel, may be found in Ref. 3.

Spreads. The *spread*, or second centralized moment, of a distribution is a standard characterizing parameter. For an instantaneous (i.e., snapshot, or unaveraged) channel distribution function, the instantaneous spread is the standard deviation of that function. For example, for a channel with a snapshot transfer function $h(\tau)$, the definition of the *instantaneous delay spread* is

$$\sigma_\tau^{(\mathrm{i})} = \sqrt{\frac{\int \tau^2 \left|h(\tau)\right|^2 \, d\tau}{\int \left|h(\tau)\right|^2 \, d\tau} - \left(\frac{\int \tau \left|h(\tau)\right|^2 \, d\tau}{\int \left|h(\tau)\right|^2 \, d\tau}\right)^2} \tag{41}$$

The (average) *delay spread*, denoted σ_τ, follows the same definition but uses the averaged distribution $P(\tau) = \langle |h(\tau)|^2 \rangle$ instead of $|h(\tau)|^2$. The analogous definition for the *Doppler spread* is

$$\sigma_u = \sqrt{\frac{\int u^2 P(u) \, du}{\int P(u) \, du} - \left(\frac{\int u P(u) \, du}{\int P(u) \, du}\right)^2} \tag{42}$$

It is important to note that it is the individual power distributions that are averaged to produce the power profiles, which are then used to produce the spreads. It is wrong to calculate the spreads of individual channels, average these, and call the result the average spread.

Power Profile Examples. Two power profiles that are commonly used for modeling because of their simplicity, are the one-sided exponential,

$$P(\tau) = \frac{1}{\sigma_\tau} \exp\left(\sqrt[\tau]{\sigma_\tau}\right) \Leftrightarrow S_H(\Delta\omega) = \frac{1}{1 + j2\pi \, \Delta\omega \, \sigma_\tau}, \qquad \tau \geq 0 \tag{43}$$

and the two-path,

$$\begin{aligned} P(\tau) &= \delta(\tau) + \left|a_2 \, \exp(j\alpha_2)\right|^2 \delta(\tau - \tau_2) \\ &\Leftrightarrow \quad S_H(\Delta\omega) = 1 + \left|a_2 \, \exp(j\alpha_2)\right|^2 \exp(-j4\pi \, \Delta\omega \, s) \end{aligned} \tag{44}$$

which are shown in Fig. 7. The exponential is the most commonly used model.

The two-path model offers much insight into the mechanisms of the channel and is used in the following to develop the basic characteristics and parameters of interest of the mobile channel's behavior. It is later extended to the many-path situation. Liberties are taken with the mathematical use of the delta functions to allow convenient modeling.

The Two-Path Model

The two-path model and its "statistics" (the model is treated statistically despite the situation being deterministic) produce and explain nearly all of the behavior that can be found in real world mobile channels. Such a model is also used in point-to-point communications where there can be a direct wave with a single ground bounce. The term "two-path" refers to two effective sources. However, the introduction of the directions of the effective sources is delayed until later, since the directions have no bearing on the received signal while the

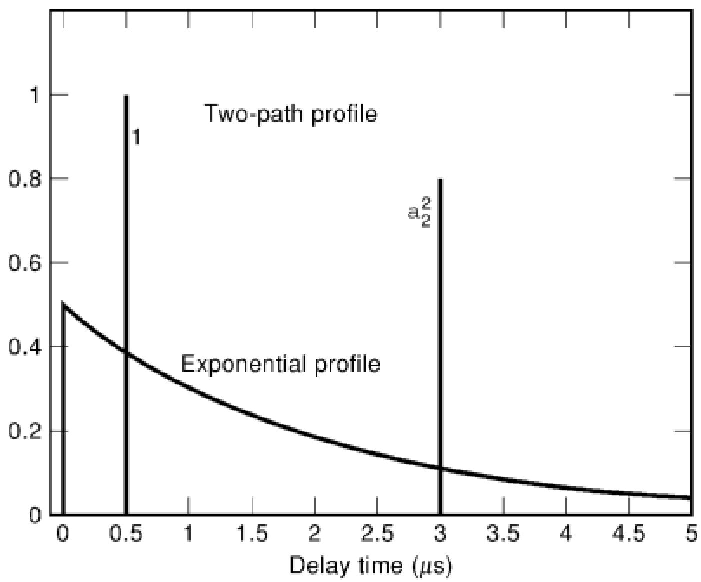

Fig. 7. Examples of the exponential and the two-path models for the power delay profile. The two-path model comprises discrete multipath contributions, whereas the exponential profile has a continuum of multipath contributions.

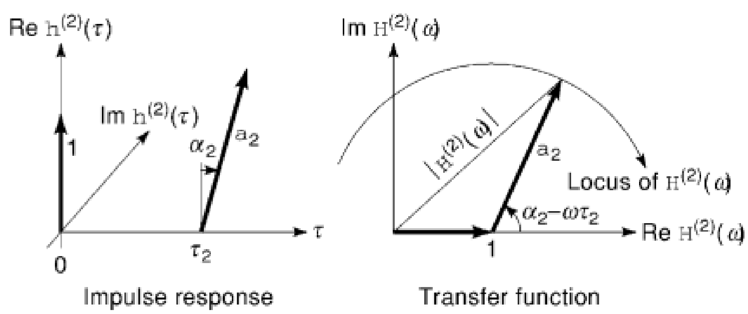

Fig. 8. The impulse response of the static two-path model amplitudes 1 and a_2, and a complex plane representation of the transfer function for the case $a_2 > 1$.

receiver is static. The moving receiver introduces a changing frequency dependence, and the rate of change is determined by the directions. Understanding the behavior of the static model allows a smooth transition to understanding the many-path channel behavior.

Static Model for Frequency-Selective Fading. The two-path scenario is shown with its variation with frequency in Fig. 8. The impulse response, on setting $\tau_1 = 0$ and $\alpha_1 = 0$ for the first path, is

$$h^{(2)}(\tau) = \delta(\tau) + a_2\ \exp(\alpha_2)\ \delta(\tau - \tau_2) \qquad (45)$$

and so represents a signal arriving with zero delay with normalized magnitude and zero phase, and a signal arriving at a delay of τ_2 with magnitude a_2 and phase α_2. The transfer function is minimum phase when $a_2 \leq 1$, and is maximum phase when $a_2 > 1$.

This model, being static in the sense that the two effective scatterers are constant in amplitude and phase, needs no averaging to obtain the power profile. So $P(\tau) = \langle\ |h(\tau)|^2\rangle = |h(\tau)|^2$ for the static case. The delay spread is thus the same as the instantaneous delay spread, and from Eqs. (44) and (41), is $\sigma_\tau^{(2)} = a_2\tau_2/(1 + a^2{}_2)$. The delay spread is not affected by time reversal or magnitude scaling of the power profile. In the two-path case, this means that a_2 can be replaced by $1/a_2$ (i.e., a change from a minimum- to a maximum-phase channel) and the delay spread stays the same.

Transfer Function. The transfer function is obtained by Fourier transformation of Eq. (45), and is (the factor $1/2\pi$ is omitted for brevity)

$$H^{(2)}(\omega) = 1 + a_2\ \exp(\alpha_2 - j\omega\tau_2) \tag{46}$$

where the delay difference is $\Delta\tau = \tau_2 - \tau_1 = \tau_2$. The in-phase component is the real part of the transfer function, $I(\omega) = 1 + a_2\ \cos(\omega\tau_2 - \alpha_2)$, and similarly the quadrature part is $Q(\omega) = a_2\ \sin(\omega\tau_2 - \alpha_2)$. Apart from the dc term, these are simply quadrature sinusoids with different amplitudes. The phase of the second effective scatterer, α_2, is now set to zero for brevity. The power transfer function is $|H\ (\omega)|^2 = 1 + a^2{}_2 + 2a_2\ \cos(\omega\ \tau_2)$, and so the frequency fading behavior is periodic with period $1/\tau_2$ (Hz). The phase of the transfer function is

$$\phi^{(2)}(\omega) = \tan^{-1}\left(\frac{-a_2\ \sin\ \omega\tau_2}{1 + a_2\ \cos\ \omega\tau_2}\right) \tag{47}$$

which has a maximum rate of change when the power is a minimum. For the case $a_2 \leq 1$, the maximum and minimum values of the phase are $\pm\sin^{-1} a_2$. When $a_2 = 1$ and $\omega\tau_2 = n\pi$ (n is an integer), the phase changes by π.

Group Delay. The group delay of a transfer function is the negative derivative of the phase with respect to frequency, $\tau_g(\omega) = -\partial\phi(\omega)/\partial\omega$. It approximates the time delay of the envelope of a narrowband signal after it has passed through a transfer function with phase $\phi\ (\omega)$ (5). Changes in the group delay mean changes in the expected arrival times of information, such as symbols, at the receiver.

For a channel that contains many delay values, the received signal becomes distorted owing to the dispersion. For the two-path model, the group delay is found by differentiating Eq. (47) to be

$$\tau_g^{(2)}(\omega) = \frac{a_2\tau_2(a_2 + \cos\ \omega\tau_2)}{1 + a_2^2 + 2a_2\ \cos\ \omega\tau_2}. \tag{48}$$

For the minimum phase case, this varies between $a_2\tau_2/(a_2 - 1)$ and $a_2\tau_2/(a_2 + 1)$. If different frequencies were sent through the channel, then these values are the extrema of the group delays that would be experienced. Figure 9 shows the in-phase and quadrature signals, the envelope and phase, and the group delay for the transfer function of a static two-path model.

Fearesf the Static Two-Path Model. The features from this deterministic model are frequency dependence with:

- Smoothly varying in-phase and quadrature components
- Fading envelope
- Sharp transitions of the phase of the transfer function, occurring when the envelope is at a minimum
- Possibility of both minimum-phase fades ($a_2 \leq 1$) and non-minimum-phase fades ($a_2 > 1$)
- Dispersive channel with sharp spikes in the group delay at the envelope minima

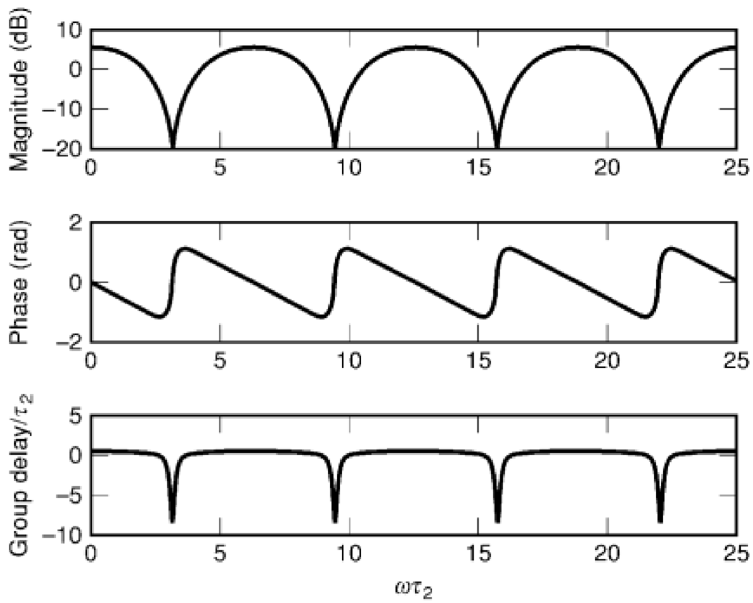

Fig. 9. The periodic frequency selective channel behavior for the static two-path model. The receiver is at a fixed position. The magnitude shows fading, the phase is changing quickly at the fade frequencies, and the group delay is correspondingly large (and negative for $a_2 \le 1$) at the fade frequencies.

These transfer function variations are all periodic in the two-path model, but as seen below, the same effects occur also in the real world channel, but with a random frequency and space dependence.

The reason for the phase behavior coinciding with the envelope is best seen from the locus of the signal in Fig. 8, where the envelope minima occur as the locus is passing closest to the origin, which is also when the phase is changing the quickest. For deep fades, the phase change is always nearly $\pm\pi$ (the sign depends on whether a_2 is less than or greater than zero), and such phase jumps are also a characteristic of the many-path channel.

Moving Receiver. In a moving receiver, we can fix the frequency to a CW for simplicity and get behavior as in the static channel of Fig. 8, but with spatial (i.e., time, for a given mobile speed), instead of frequency, dependence. For a CW channel, the transfer function is

$$H^{(2)}(z) = 1 + a_2 \ \exp(\alpha_2 + \Delta u\, z) \tag{49}$$

where $\Delta u = k_{\rm C}(\cos\,\theta_2 - \cos\,\theta_1)$ is the spatial Doppler frequency difference between the two effective sources. The transfer function now has spatial periodicity with a period (in meters) of $2\pi/\Delta u$. For example, with sources exactly in front of ($\theta_1 = 0$) and behind ($\theta_2 = \pi$) the moving receiver, the periodicity is given by a spacing of exactly $z = \lambda_{\rm C}/2$, that is, half the carrier wavelength.

Random Frequency Modulation. The spatial analogy to the group delay is the random FM, given in radians per meter by the derivative of the phase with respect to position as $\omega_{\rm R}(z) = 2\pi\ \partial\phi(z)/\partial z$. The random FM is an angle modulation in the channel and will be applied to a signal borne by the channel. It means that angle-modulation systems are affected as the receiver moves. In practice, the random FM is often too small to be noticed in a working system, but as carrier frequencies increase, the fading rate and the spectrum of random FM increasingly invades the signal band. In summary, the CW spatial mobile channel follows the same behavior as that in the frequency-dependent static channel, the transfer function signals shown in

Fig. 9. apply with the abscissa $\omega\tau_2$ replaced with $z\ \Delta u$, and the group delay becomes the random FM (with the opposite polarity).

Two-Dimensional Transfer Function. The frequency and spatial dependences can be combined to give the two-dimensional transfer function, again with $\alpha_2 = 0$,

$$H^{(2)}(\omega, z) = 1 + a_2\ \exp(\Delta u\, z - \omega\tau_2) \qquad (50)$$

which explicitly indicates the two-dimensional nature of the fading. The range of angles, Δu, determines the spatial fading rate, and the range of delay times, $\Delta\tau = \tau_2$, determines the rate of fading in the frequency domain. The statistical equivalents of these quantities, the Doppler spread and the delay spread, are used for describing the average fading rates found in the real world many-path situation.

Statistical Approach Using Two-Path Model

The statistical approach is required when there are too many paths to determine the channel, which is normally the case in mobile communications. The statistical approach to the two-path model also offers insight into the statistical behavior of the many-path case. In the static case, the transfer function of the two-path model assumes all its possible values as the relative amplitude a_2 and phase α_2 are varied. In practice, averaging is over the phase-mixing process, so here we fix the amplitude and average over the changing phase only. In the static case, the phase of the frequency-dependent transfer function can be changed by changing the frequency. In a mobile channel, the fixed-frequency transfer function is averaged over the varying phase by averaging over many positions.

Since the two-path transfer function has a symmetric, periodic envelope with half period π/τ_2 (rad), equally likely frequencies are expressed by a uniform probability density function (*pdf*) over one of the periods,

$$p_\omega(\omega) = \frac{\tau_2}{\pi}, \qquad n\frac{\pi}{\tau_2} \le \omega \le (2n+1)\frac{\pi}{\tau_2} \qquad (n \text{ any integer}) \qquad (51)$$

The analogous expression for the moving receiver holds for equally likely positions, viz., $p_z(z) = \Delta u/\pi$. These pdfs allow the pdfs of the channel function to be calculated below.

Probability Density Function of Channel Power. For $a_2 < 1$ and equally likely frequencies, the pdf for the power $\gamma(\omega) = |H(\omega)|^2$ is, from function transformation of p_ω,

$$p_\gamma^{(2)}(\gamma) = p_\omega(\omega)\left|\frac{\partial\omega}{\partial\gamma(\omega)}\right| = \frac{1}{\pi\sqrt{(2a_2)^2 - [\gamma - (1+a_2^2)]^2}} \qquad (52)$$

where $1 + {a_2}^2$ and $(2a_2)^2$ are the mean and variance respectively of the power in the two-path channel.

Cumulative Probability Function of Channel Power. The cumulative probability function (*cpf*) is the integral of the pdf over its range of values $(1-a_2)^2$ to $(1 + a_2)^2$, and is written

$$P_\gamma^{(2)}(\gamma^{(2)}(\omega) \le \gamma_0) = 1 - \frac{1}{\pi}\cos^{-1}\left(\frac{\gamma_0 - (1+a_2^2)}{2a_2}\right) \qquad (53)$$

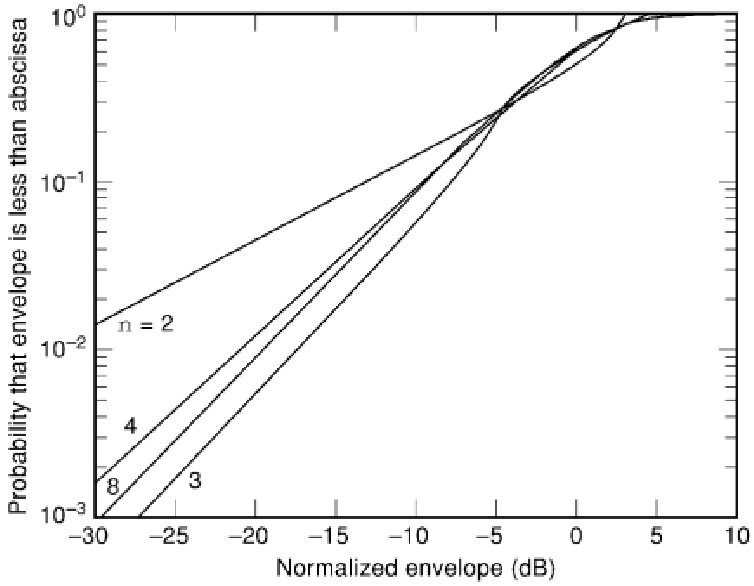

Fig. 10. The cpf for the power of the $n = 2, 3, 4, 8$ channels, where all the multipath amplitudes are the same. The $n = 8$ model is essentially the same, for the cpf range displayed, as Rayleigh ($n \to \infty$) distribution, given in Fig. 14.

This probability approach is an alternative to the deterministic form $H^2(\omega)$ for characterizing the two-path channel. The approach is needed when a deterministic form is not available. The cpfs for the n-path model with all the $a_n = 1$ are given in Fig. 10 for $n = 2$, 3, and 8. The 8-path case is very close, except at the tails of the distribution, to the Rayleigh distribution, which corresponds to the limiting case $n \to \infty$, discussed further below.

The pdf for the two-path case is centered at its mean, $1 + {a_2}^2$, and is confined to its limits, that is, between $(1 - a_2)^2$ and $(1 + a_2)^2$. At these limits, the pdf ${p_\gamma}^2$ goes to infinity. The many-path pdfs can behave the same way. This does not cause interpretation problems, however, since the probability of the power being at these limits is infinitesimal and the integral of the function of course maintains its unity value. For example, for $a_2 = 1$, the fades go exactly to zero in the transfer function. In the cpf of Fig. 10, the interpretation is that there is an infinitesimally small probability of the power being zero, that is,:

$$P(\gamma(\omega) \leq \gamma_0) \to 0 \quad \text{as} \quad \gamma_0 \to 0, \qquad a_2 = 1 \tag{54}$$

A similar situation holds for the power approaching its maximum value $(1 + a_2)^2$:

$$P(\gamma(\omega) \leq \gamma_0) \to 1 \quad \text{as} \quad \gamma_0 \to (1 + a_2)^2 \tag{55}$$

In the $a_2 = 1$ two-path example, the cpf diagram shows that for 10% of the frequencies the power transfer function is more than 13 dB below its mean value. The cpf curves are arranged so that the mean power always corresponds to 0 dB. A flat channel ($a_2 = 0$) would be represented by a line at $\gamma_0 = 0$ dB.

In summary, it is the phase difference between the source contributions that is the generic random variable for the statistical approach to the short-term variation of the power or envelope. In the static scenario, the averaging over the phase difference is implemented by varying the frequency. For the moving receiver case,

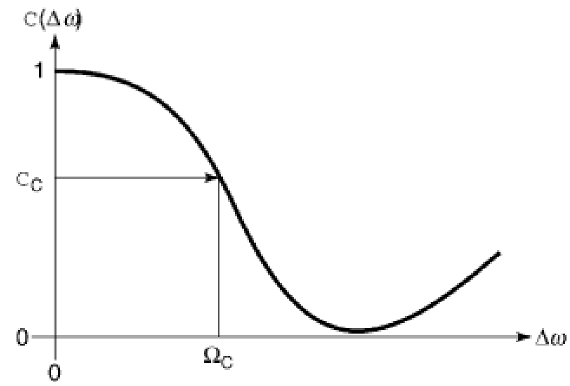

Fig. 11. The definition of a coherence bandwidth, Ω_C, in terms of the frequency correlation coefficient function, or coherence function, and a correlation value of C_C. Narrowband channels, separated by a minimum frequency Ω_C, will display mutually uncorrelated fading in the sense that the correlation coefficient is $C_c < \sim 0.75$.

the CW transfer function is averaged over space. In the general case, the transfer function is a two-dimensional distribution with phase mixing causing fading in both frequency and position.

Coherence Bandwidth. An important parameter in a frequency-selective fading channel is the frequency separation for which the fading becomes effectively independent in the statistical sense. This frequency separation is determined by the autocorrelation of the channel transfer function. It is presented here as independent of frequency, that is, the channel is assumed to be WSS. The frequency correlation coefficient function, sometes referred to as the coherence function, is

$$C(\Delta\omega) = \frac{S_H(\Delta\omega) - \langle H(\omega)\rangle \langle H^*(\omega)\rangle}{S_H(0) - \langle H(\omega)\rangle \langle H^*(\omega)\rangle} \tag{56}$$

and for the static two-path model with $a_2 = 1$, the magnitude of this is

$$\left| C^{(2)}(\Delta\omega) \right| = \left| \cos \frac{\Delta\omega\, \tau_2}{2} \right|, \qquad a_2 = 1 \tag{57}$$

The coherence bandwidth Ω_C (rad/s) is defined as the frequency span from the maximum (unity) of the frequency correlation coefficient function to where the magnitude of the function first drops to a value C_C, that is,

$$|C(\Delta\omega = \Omega_C)| = C_C \tag{58}$$

as illustrated in Fig. 11.

C_C is taken by various authors from $1/e = 0.37$ to 0.9 (6,7,8). A change of C_C scales the coherence bandwidth nonlinearly, so any results derived from some value of C_C are also scaled in some way. The coherence function is periodic in $\Delta\omega$ for the two-path channel, since $H^{(2)}\omega$ is periodic. $\Omega^{(2)}{}_C$ minimum for $a_2 = 1$, and for this case, the coherence bandwidth in hertz, $\Omega^{(2)}{}_C/2\pi$, can be written directly from Eqs. (57) and (58) as

$$B^{(2)}_{C,\mathrm{Hz}} = \frac{1}{\pi\, \tau_2} \cos^{-1} C_C, \qquad a_2 = 1 \tag{59}$$

The coherence bandwidth decreases with increasing delay difference between the two-path contributions, τ_2. Also, the coherence bandwidth decreases with increasing relative amplitude a_2. When a_2 is small, the coherence bandwidth becomes undefined, as the coherence function does not drop down to C_C .

Product of Coherence Bandwidth and Delay Spread. While the delay spread is a measure of the channel time dispersion, the coherence bandwidth is a measure of the fading rate with changing frequency. The ideal communications channel has a zero delay spread and infinite coherence bandwidth. For the two-path model, the delay spread increases while the coherence bandwidth decreases for increasing relative delay τ_2 and increasing relative amplitude a_2. The coherence bandwidth and the delay spread are thus inversely related, but the exact relationship is not simple in the many-path case.

The product of these two parameters was taken for experimental channels using $C_C = 0.75$ (7), and an empirical law was found that $B\sigma_\tau$ was constant and approximately equal to 1/8 (Gans's law). The constancy of the product can also be viewed as an uncertainty principle (5,9). It gives a lower bound for the many-path channel as

$$B_{C,Hz}(C_C) \cdot \sigma_\tau \geq \frac{1}{2\pi} \cos^{-1} C_C \qquad (60)$$

The equality holds for the two-path case with equal powers, as in Eq. (59), which corresponds to maximum delay spread.

For the two-path channel, the product $B_C{}^{(2)}\sigma_T{}^{(2)}$ does not exist. The dependence of this product on a_2, is weaker than its dependence on the choice of C_C. The product $B_C{}^{(2)}\sigma_\tau{}^{(2)}$ is a minimum when a_2 is 1, that is, when the frequency fades are the deepest. In this case and for the value $C_C = 0.75$, the two-path product is in close agreement with Gans's law, $B_{C,Hz}{}^{(2)}\sigma_\tau{}^{(2)} = (1/2\pi) \cos^{-1} 0.75 \approx \frac{1}{8}$.

In the two-path model, then, the virtually constant value of the product allows the delay spread to be calculated from a measured correlation bandwidth, or vice versa. However, in a general many-path case, the expression for the coherence-bandwidth–delay-spread product must be heeded as a lower limit. It should always be borne in mind that the choice of C_C for the coherence bandwidth affects the value of the product. Because the delay spread is mathematically unbounded in the model (no limit is placed on τ_2), there is no theoretical upper limit for $B\sigma_\tau$ in the many-path case, even though the coherence bandwidth can simultaneously remain essentially constant. In practice, physical and practical considerations such as the space loss described below are imposed on the model and the delay spread and the product become bounded through these.

Correlation Distance. The correlation distance is the spatial counterpart of the coherence bandwidth. It is traditionally defined as the spatial displacement $d_d = \Delta z$ corresponding to when the spatial correlation coefficient, defined at a given frequency, decreases to some value. Instead of using the complex transfer function *H(z)*, analogously to using $H(\omega)$ for the coherence function, the envelope correlation coefficient function,

$$\rho_r(\Delta z) = \frac{R_r(\Delta z) - \langle r \rangle^2}{R_r(0) - \langle r \rangle^2} \qquad (61)$$

has been used traditionally, and the coefficient value is taken as $\rho r(d_d) = 0.7$. The correlation distance is a measure of the spatial fading rate and therefore depends inversely on the spatial Doppler spread σu. The product of these, d_d σu, is lower bounded, but not with the same relationships as $B\sigma_\tau$.

MAny-Path Model

The above discussion has touched several times on the many-path model. Many channel parameters for the three-path model can be derived deterministically. The three-path model has been of interest in point-to-point links because it matches the physical situation of a direct, a ground bounce, and a single atmospherically diffracted ray. It has been also used to help "randomize," relative to the two-path model, a transfer function for a more realistic-looking (over two or three fades), but tractable, model. However, it otherwise offers little more insight into the channel behavior than does the two-path model. The statistics for the few-path (less than about 10) less than about) model are rather complicated. When there are more than about 10 components of similar amplitude, however, the statistics follow, to a good approximation, the limiting case of a very large number of paths. The phase-mixing process of adding many random phasors gives, from the central limit theorem, the classical Rayleigh channel. The distribution functions are given below.

Phase Mixing with Many Random Contributions. Equations (11) and (12) describe the model. For a narrow band channel, the in-phase and quadrature components are Gaussian distributed from the central limit theorem. It follows that: the distribution of the power is chi-square with two degrees of freedom (i.e., exponential), the envelope is Rayleigh-distributed, and the phase is uniformly distributed. The transfer function signals, as a function of position, are depicted in Fig. 12. The incident power is from all directions for this example. The figure can be compared with the signals from the two-path model, shown as a function of frequency in Fig. 9. The features of the channel are essentially the same as those in the two-path model, although the process is random. There are both minimum-phase and maximum-phase deep fades. Similarly, the random FM spikes have an associated polarity that is random.

Rayleigh Envelope and Uniform Phase. The signal representing the channel transfer function is represented as a complex Gaussian process. The in-phase component and quadrature components are denoted x and y, the envelope r, and the phase θ, and these are related as

$$x + jy = r\,e^{j\theta} \tag{62}$$

Here x and y are independent, zero mean Gaussians, so the pdf for each is (here for x)

$$p_x(x) = \frac{1}{\sqrt{2\pi}\,\sigma}\exp\left(-\frac{x^2}{2\sigma^2}\right) \tag{63}$$

where σ is the standard deviation of each component. The envelope and phase pdfs are established as independent with Rayleigh and uniform distributions respectively, through the steps

$$\begin{aligned} p_{r,\theta}(r,\,\theta) &= p_{x,\,y}(x,\,y)\left|\frac{\delta(x,\,y)}{\delta(r,\,\theta)}\right| \\ &= \frac{r}{\sigma^2}\exp\left(\frac{-r^2}{2\sigma^2}\right)\cdot\frac{1}{2\pi} \qquad (r \geq 0) \\ &= p_r(r)\cdot p_\theta(\theta) \end{aligned} \tag{64}$$

The pdf of the phase is $1/(2\pi)$, so the mean phase is π and the standard deviation is $\pi/3$. The averaged power is

$$\langle r^2\rangle = \langle x^2\rangle + \langle y^2\rangle = 2\sigma^2 \tag{65}$$

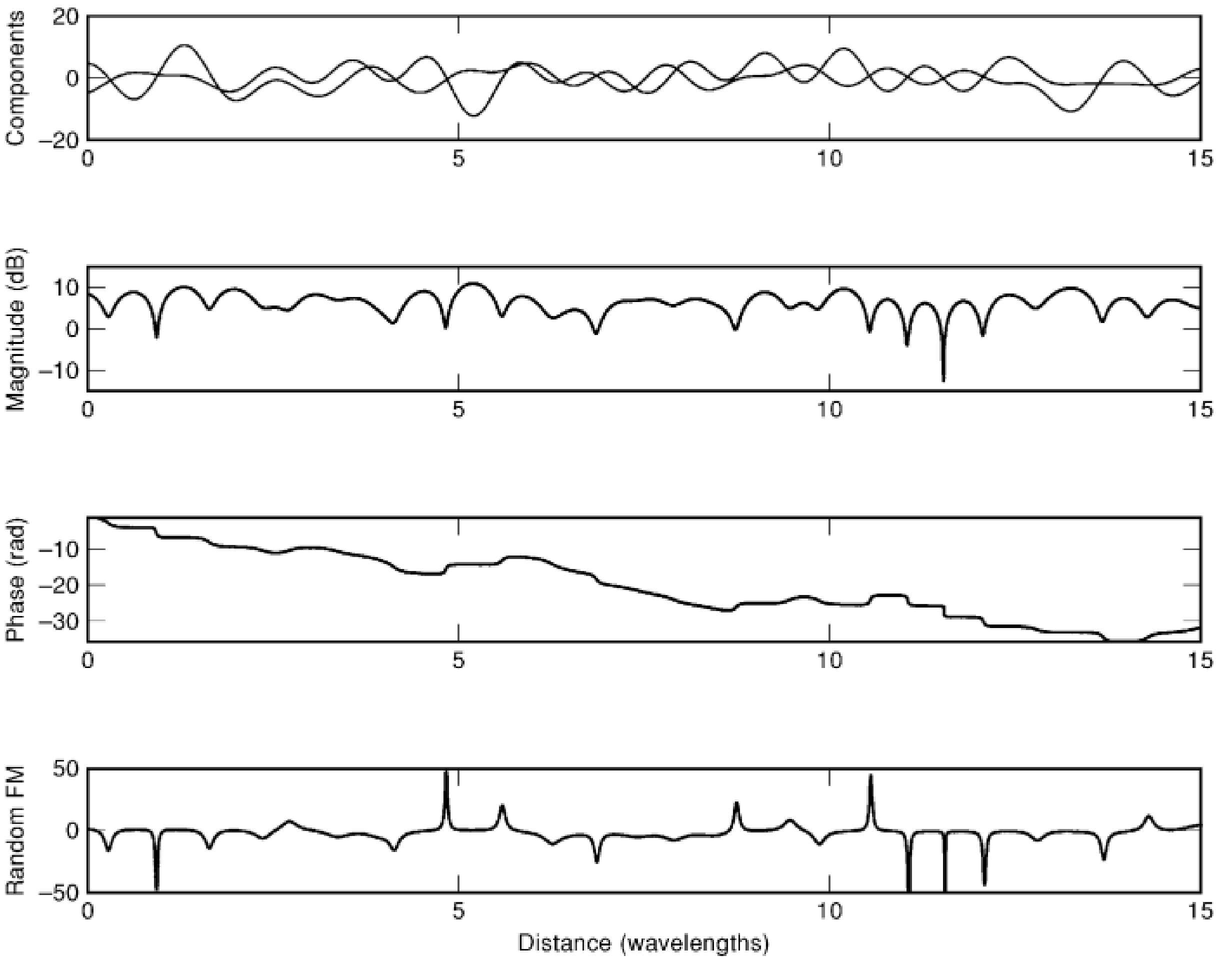

Fig. 12. The signals of a many-path, narrowband channel as a function of position. As the mobile receiver moves, the narrowband signal quantities vary in a way similar to the behavior of the plots. The in-phase and quadrature components comprise complex Gaussians, the magnitude or envelope is Rayleigh-distributed, the phase is uniformly distributed, and the random FM is Student-t distributed.

and r^2 is recognized as having a chi-square distribution with two degrees of freedom,

$$p_{r^2}(r^2) = \frac{1}{2\sigma^2} \exp\left(-\frac{r^2}{2\sigma^2}\right) \tag{66}$$

The Rayleigh statistics are included in the more general Rice statistics, below.

Rice Envelope and Phase. Sometimes, there is a single dominant effective source. This usually corresponds to a line-of-sight situation, which gives a single dominant effective scatterer. Multipath transmission still occurs, and the Rice distribution describes the statistics of the narrowband envelope. The Rice distribution results from one or both of the Gaussian processes having nonzero mean. These

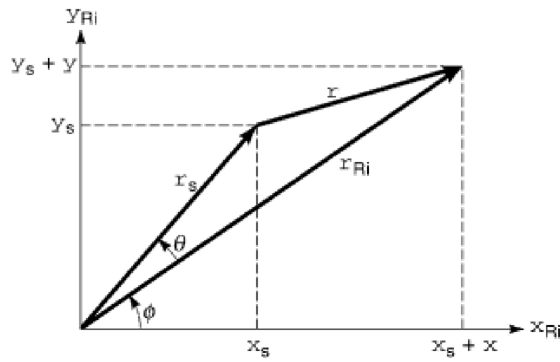

Fig. 13. The Rice process has envelope r_{Ri} comprising the additive constant r_s and the Rayleigh envelope r. The phase of the Rice signal is θ.

phase processes become

$$x_{\mathrm{Ri}} = x + x_s, \quad y_{\mathrm{Ri}} = y + y_s \tag{67}$$

where the x and y are zero-mean Gaussian and x_s and y_s are the respective means representing the dominant component (sometimes called the *specular*, or *coherent* component, with x and y representing the *diffuse*, or *incoherent* component) of the signal. The phasor combination is shown in Fig. 13. in which $\phi = \tan^{-1}(y_{\mathrm{Ri}}/x_{\mathrm{Ri}})$ is the absolute phase of the Rice envelope r_{Ri}, and θ_{Ri} is the phase difference between r_{Ri} (Rayleigh component plus dominant component) and the dominant component r_s. The mean of the absolute phase of the process is $(\theta_{\mathrm{Ri}} + \phi)$. A coordinate rotation allows the phase to bdefined as just θ_{Ri}.

From

$$(x_{\mathrm{Ri}} - x_s)^2 + (y_{\mathrm{Ri}} - y_s)^2 = r^2 = r_{\mathrm{Ri}}^2 + r_s^2 - 2r_{\mathrm{Ri}}r_s \cos\theta_{\mathrm{Ri}} \tag{68}$$

the Rice pdf is

$$p_{r_{\mathrm{Ri}},\theta}(r_{\mathrm{Ri}}, \theta) = \frac{r_{\mathrm{Ri}}}{2\pi\sigma^2} \exp\left(-\frac{r_{\mathrm{Ri}}^2 + r_s^2 - 2r_{\mathrm{Ri}}r_s \cos\theta}{2\sigma^2}\right) \tag{69}$$

The envelope and phase are thus statistically dependent, unlike the Rayleigh case. The $+\pi$ and $-\pi$ transitions that occur in the phase of the Rayleigh signal as the locus passes near the origin are now reduced to smaller values, which depend on the length of the envelope phasor component r_{Ri}. The Rice channel can be purely minimum phase when the dominant component is large enough.

The Rice k factor is the ratio of powers of the dominant component and the Rayleigh component,

$$k_{\mathrm{Ri}} = \frac{r_s^2}{2\sigma^2} \tag{70}$$

When the dominant component r_s approaches zero, k_{Ri} approaches 0, and the distribution reduces to Rayleigh. Similarly, when the dominant component becomes very large, the Rice distribution for the envelope approaches Gaussian with mean r_s.

Rice Envelope. For convenience, the envelope is normalized by the Gaussian standard deviation:

$$r_{\mathrm{Ri}}^{(\mathrm{n})} = \frac{r_{\mathrm{Ri}}}{\sigma} \tag{71}$$

The envelope pdf is

$$\begin{aligned} p_{r_{\mathrm{Ri}}}(r_{\mathrm{Ri}}) &= \frac{r_{\mathrm{Ri}}}{2\pi\sigma^2}\ \exp\left(-\frac{r_{\mathrm{Ri}}^2+r_{\mathrm{s}}^2}{2\sigma^2}\right)\int_0^{2\pi}\exp\left(\frac{r_{\mathrm{Ri}}r_{\mathrm{s}}\ \cos\ \theta}{\sigma^2}\right)d\theta \\ &= \frac{r_{\mathrm{Ri}}}{\sigma^2}\ \exp\left(-\frac{r_{\mathrm{Ri}}^2+r_{\mathrm{s}}^2}{2\sigma^2}\right)I_0\left(\frac{r_{\mathrm{Ri}}r_{\mathrm{s}}}{\sigma^2}\right), \qquad r_{\mathrm{Ri}} \ge 0 \end{aligned} \tag{72}$$

or

$$\begin{aligned} &p_{r_{\mathrm{Ri}}^{(\mathrm{n})}}(r_{\mathrm{Ri}}^{(\mathrm{n})}) \\ &= \frac{1}{\sigma}r_{\mathrm{Ri}}^{(\mathrm{n})}\ \exp\left\{-\left[\frac{1}{2}\left(r_{\mathrm{Ri}}^{(\mathrm{n})}\right)^2+k_{\mathrm{Ri}}\right]\right\}\ I_0\left(r_{\mathrm{Ri}}^{(\mathrm{n})}\sqrt{2k_{\mathrm{Ri}}}\right), r_{\mathrm{Ri}}^{(\mathrm{n})} \ge 0 \end{aligned} \tag{73}$$

As k_{Ri} approaches infinity, the Rice pdf becomes a delta-like function, being a Gaussian with a variance approaching zero.

The Rice distribution is sometimes called Nakagami–Rice, in recognition of its independent development by Rice (10) and by Nakagami (11), who reported it in English at a later time. Because of its physical justification for many situations, the Rice distribution is the preferred one for short-term fading. Review material covering aspects of Rice's work is in Refs. 12,13. The distribution for the random FM and group delay for the Rice channel is given by the Student t distribution (14).

The Rice envelope cumulative probability function (*cpf*) is expressed as

$$P_{r_{\mathrm{Ri}}}(r_0) = \mathrm{Prob}(r_{\mathrm{Ri}} \le r_0) = 1 - Q_1\left(\frac{r_{\mathrm{s}}}{\sigma}, \frac{r_0}{\sigma}\right) \tag{74}$$

where Q is the Marcum Q function (15). Further worthwhile discussion on the Q function is given in Refs. 16,17. The Rice envelope cpf is sketched in Fig. 14. for values of the Rice k factor, including the Rayleigh case.

Lognormal Shadow Fading. Shadow fading has been found experimentally to be well described by the lognormal distribution. Whereas the Gaussian distribution results from the addition of many random variables, the lognormal distribution results from the product of many positive random variables. It follows that when Gaussian variables are expressed in logarithmic units, they then follow a lognormal distribution. The transformation of variables between the distributions is $z = e^{x}$, or $\ln z = x$. (z here is a variable, not distance.) If x is Gaussian, then z is lognormal. Alternatively stated, if z is lognormal, then $\ln z$ is Gaussian. The pdf of the lognormal distribution is found from the Gaussian pdf, viz.,

$$p_{\mathrm{l}}(z) = p_x(x)\left|\frac{\partial x}{\partial z}\right| = \frac{1}{\sqrt{2\pi}\sigma_{\mathrm{l}z}z}\ \exp\left(-\frac{(\ln z - m_{\mathrm{l}z})^2}{2\sigma_{\mathrm{l}z}^2}\right) \tag{75}$$

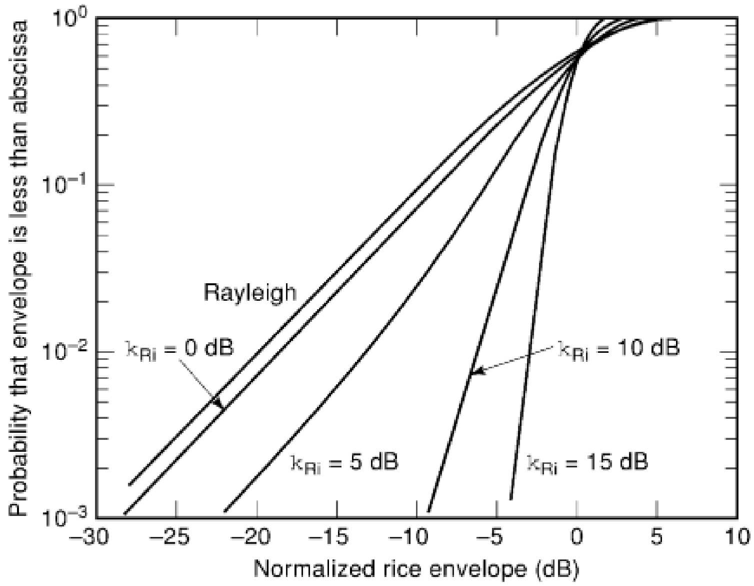

Fig. 14. The Rice envelope cpf. For zero specular component, the distribution is Rayleigh, and approaches Gaussian (vertical line at 0 dB) for an asymptotically large specular component.

where m_{lz} and $\sigma_{\mathrm{lz}}{}^2$ are the mean and variance respectively of $\ln z$. The lognormal signal representing the local mean of the envelope looks like one of the phase components of Fig. 14, except that the scale would be in decibels rather than linear. Typically σ_{lz} is 3 dB to 8 dB in urban environments.

Suzuki: Lognormal and Rayleigh. Combining the short-term Rayleigh and long-term lognormal distributions provides a model for the stochastic component of the path loss of a narrowband signal in mobile communications.

The lognormal distribution is over the mean of the envelope. This can be interpreted as Gaussian for the envelope mean in decibels. The Rayleigh envelope mean is linearly related to the Gaussian standard deviation, viz., $\langle r \rangle = \sqrt{\pi/2\sigma}$, so the lognormal distribution can be applied to the σ (18). The distribution can be written

$$p_{\mathrm{Su}}(r) = \int_0^{\infty} \frac{r}{\sigma^2} \exp\left(-\frac{r^2}{2\sigma^2}\right) \cdot \frac{1}{\sqrt{2\pi}\sigma\sigma_{\mathrm{l}}} \exp\left(-\frac{(\ln\sigma - m_{\mathrm{l}})^2}{2\sigma_{\mathrm{l}}^2}\right) d\sigma \tag{76}$$

No closed form has been found for the integral, which is a practical inconvenience when applying the Suzuki distribution. However, the distribution has the advantage of being based on a physical model for the envelope, and thus offers good agreement with experimental results on large scale records of envelopes of narrowband signals.

Many other distributions have been used to fit mobile channel fading (19). Some have various advantages for mathematical manipulations or for the fitting of experimental data. Two are noteworthy because of their versatility. The Nakagami m (11) distribution has a single parameter that allows the shape of the distribution to be altered, in particular for small values of r. The generalized gamma distribution (20) has effectively two parameters that can independently adjust the shape of the small and large values of r.

Path Loss and the Mobile Channel

Much of the above discussion has been a statistical description of the behavior of the mobile channel. The interest in the envelope or power of the mobile transfer function is because this dominates the SNR of the received signal. The power is also referred to as the channel gain. How this ties in with the path loss is addressed in this section. In so doing, the discussion returns to the electromagnetic propagation and antenna issues of the opening sections.

The path loss is a well-defined concept originating from point-to-point radio links. It comes from the Friis transmission equation, which relates the transmitted and received powers (P_{T}, P_{R} respectively), the antenna gains (G_{T}, G_{R} respectively), and the path loss L:

$$\frac{P_{\mathrm{R}}}{P_{\mathrm{T}}} = G_{\mathrm{T}} G_{\mathrm{R}} \frac{1}{L} \tag{77}$$

The path loss is seen from this equation to be the reciprocal of the path gain. For frequency-independent antenna gains, the free space path loss for a separation distance d and wavelength $\lambda = c/f$ is

$$L_{\mathrm{F}} = \left(\frac{4\pi d}{\lambda}\right)^2 = \left(\frac{4\pi f d}{c}\right)^2 \tag{78}$$

so that it varies as the frequency squared and the distance squared. The incident field strength is not dependent on frequency. In Eq. (78), the antennas are considered impedance- and polarization-matched.

Mean Path Loss and Mean Antenna Gain. In a mobile channel, the classical point-to-point situation does not apply. The received power and the receiving antenna gain become statistical quantities. The antenna's *mean gain* can be defined by the average gain into a well-defined distributed direction. The mean received power can be defined from a time average. The path loss is the time-varying quantity (because of the spatially dependent phase mixture of multipath propagation signals), and so the mean received power with Eq. (77) defines a *mean path loss*. Sometimes the term *mean effective gain* is used when comparing antennas by measuring their time-averaged received powers in the same environment. In this context, it must be assumed that the transmitting power and the mean path loss are both common to each measurement record used for the averaging. The mean effective gains are then proportional to the mean received powers and include polarization mismatches. What is being measured is how well, on average, the vector antenna pattern is directed towards the vector distribution of incoming power from the measurement environments.

Scenario Models. Model distributions are used to approximate the average incident power directions for various applications. For a mobile vehicle, for example, the Clarke scenario (21,22), given by

$$S^{(\mathrm{C})}(\theta, \phi) = S^{(\mathrm{C})}(\phi) = \frac{1}{2\pi} \delta\left(\theta - \sqrt[\pi]{2}\right) \tag{79}$$

is often used. This corresponds to a uniform source distribution at the horizon, surrounding the antea. Transforming to the spatial Doppler variable results in the pdf

$$p_u^{(\mathrm{C})}(u) = \frac{1}{\pi\sqrt{k_{\mathrm{C}}^2 - u^2}} \tag{80}$$

and this spatial Doppler spectrum is for the incident fields or the electromagnetic propagation channel (for one polarization), and also for the mobile channel if an omnidirectional (in the $\theta = \pi/2$ plane) antenna is used. The spatial Doppler spread is $\sigma_{\mathrm{u}}{}^{(\mathrm{C})} = k_{\mathrm{C}}/\sqrt{2}$ (rad/m). The spatial correlation coefficient for the envelope is $\rho_{\mathrm{r}}{}^{(\mathrm{C})}(\Delta z) \approx J_0{}^2(k_{\mathrm{C}}\ \Delta z)$, giving a 0.7-correlation distance of about 0.13 wavelengths and an average distance between fades of about 0.5 wavelengths.

For a directional antenna, the spatial Doppler distribution corresponding to the pattern must be multiplied with Eq. (80) to get the spatial Doppler spectrum of the mobile chanl. This is how the antenna pattern can control the mobile channel behavior. A single-lobed, directional pattern acts as a spatial Doppler bandpass filter and results in a decreased (relative to an omnidirectional pattern) Doppler spread, and therefore a decreased spatial fading rate. This effect can be seen with laser speckle, where the dark areas are the deep fades of energy, and the interspeckle distance, even though the frequency is optical, is sufficiently large to be visible to the eye because the spatial Doppler spread of the illuminating beam is so small.

BIBLIOGRAPHY

1. R. G. Vaughan J. Bach Andersen, *Principles of Propagation and Antennas in Mobile Communications*, London: Peregrinus, 2000.
2. T. Miki M. Hata, Performance of 16 kbits/s GMSK transmission with postdetection selection diversity in land mobile radio, *IEEE Trans. Veh. Technol.*, **VT-33** (3): 128–133, 1984.
3. K. Sakoh, *et al.* Advanced radio paging service supported by ISDN, Proc. *Nordic Seminar on Digital Land Mobile Radiocommunication*, Espoo, Finland, February 1985, pp. 239–248.
4. P. A. Bello, Characterization of randomly time-variant linear channels, *IEEE Trans. Circuits Syst.*, **CS-11**: 360–393, December 1963.
5. A. Papoulis, *Signal Analysis*, New York: McGraw-Hill, 1977.
6. P. A. Bello B. D. Nelin, The effect of frequency selective fading on the binary error probabilities of incoherent and differentially coherent matched filter receivers, *IEEE Trans. Circuits Syst.*, **CS-21**, 170–186, June 1963.
7. M. J. Gans, A power spectral theory of propagation in the mobile-radio environment, *IEEE Trans. Veh. Technol.*, **VT-21** (1): 27–38, February 1972.
8. D. C. Cox R. P. Leck, Correlation bandwidth and delay spread multipath propagation statistics for 910 MHz urban mobile radio channels, *IEEE Trans. Commun.*, **Com-23** (11): 1271–1280, 1975.
9. B. H. Fleury, An uncertainty relation for WSS processes and its application to WSSUS systems, *IEEE Trans. Commun.*, **Com-44** (12): 1632–1635, December 1996.
10. S. O. Rice, Mathematical analysis of random noise, *Bell Syst. Tech. J.*, 1944, No. 3; 1945, No. 1.
11. M. Nakagami, The *m*-distribution—a general formula of intensity distribution of rapid fading, in W. C. Hoffman (ed.), *Statistical Methods in Radio Wave Propagation*, Oxford: Permagon, 1960.
12. W. B. Davenport W. L. Root, *An Introduction to the Theory of Random Signals and Noise*, New York: McGraw-Hill, 1958; reprinted, Piscataway, NJ: IEEE Press, 1987.
13. D. Middleton, *An Introduction to Statistical Communications Theory*, New York: McGraw-Hill, 1960; reprinted, Piscataway, NJ, IEEE Press, 1997.
14. J. Bach Andersen, S. L. Lauritzen, C. Thommesen, Distributions of phase derivatives in mobile communications, *IEE Proc.*, **137** (4): 197–201, 1990.
15. J. I. Marcum, A statistical theory of target detection by pulsed radar, *IRE Trans.*, **IT-6**: 59–267, April 1960.
16. S. Stein, M. Schwartz, W. R. Bennett, S. Stein, *Communications Systems and Techniques*, New York: McGraw-Hill, 1966, Part III; reprinted, Piscataway, NJ: IEEE Press, 1996.
17. J. G. Proakis, *Digital Communications*, New York: McGraw-Hill, 1983.
18. H. Suzuki, A statistical model for urban radio propagation, *IEEE Trans. Commun.*, **Com-25** (7): 673–680, July 1977.
19. J. Griffiths J. McGeehan, Interrelationship between some statistical distributions used in radio-wave propagation, *IEE Proc.*, **129**, Part F, No. 6, 411–417, December 1982.

20. A. J. Coulson, A. G. Williamson, R. G. Vaughan, Improved fading distribution for mobile radio, *IEE Proc. Commun.*, **46**: 494–502, 1998.
21. R. H. Clarke, A Statistical theory of mobile radio reception, *Bell Syst. Tech. J.*, **47**: 957–1000, 1968.
22. W. C. Jakes (ed.), *Mobile Microwave Communications*, New York: AT&T, 1974; reprinted, Piscataway, NJ: IEEE Press, 1989.

READING LIST

W. C. Jakes (ed), *Mobile Microwave Communications*, New York: AT&T, 1974; reprinted Piscataway, NJ: IEEE Press, 1989.
W. C. Y. Lee, *Mobile Communications Engineering*, New York: McGraw-Hill, 1982.
R. C. V. Macario, *Personal and Mobile Radio Systems*, IEE Telecommunications Series, 25, London: Peregrinus, 1991.
J. D. Parsons, *The Mobile Radio Propagation Channel*, London: Pentech Press, 1992.
T. S. Rappaport, *Wireless Communications, Principles and Practice*, New York: IEEE Press, 1996.
S. O. Rice, Statistical properties of a sine wave plus random noise, *Bell Syst. Tech.*, **27**: 109–157, 1948.
R. Steele, *Mobile Radio Communications*, London: Pentech Press, 1992.
G. Stüber, *Principles of Mobile Communications*, Boston: Kluwer, 1996.
R. C. Vaughan J. Bach Andersen, *Principles of Propagation and Antennas in Mobile Communications*, London: Peregrinus, 2000.

RODNEY G. VAUGHAN
Industrial Research Limited, New Zealand